Spectroscopic Properties and Ligand Field Analysis of Pentaammine(imidazole)chromium(III) Perchlorate

Jong-Ha Choi

Department of Chemistry, Andong National University, Andong 760-749, Korea
Received September 9, 1998

The emission and excitation spectra of $[Cr(NH_3)_5(imH)](ClO_4)_3 \cdot H_2O$ (imH=imidazole) taken at 77 K are reported. The 298 K visible and far-infrared spectra are also measured. The vibrational intervals of the electronic ground state are extracted from the far-infrared and emission spectra. The ten electronic bands due to spin-allowed and spin-forbidden transitions are assigned. Using the observed transitions, a ligand field analysis has been performed to determine the bonding properties of coordinated imidazole in the title chromium(III) complex. It is confirmed that nitrogen atom of the imidazole ligand has a medium π-acceptor property toward chromium(III) ion. The zero-phonon line in the excitation spectrum splits into two components by 181 cm^{-1}, and the large ^2E_g splitting can be reproduced by the ligand field theory.

Introduction

A considerable amount of data concerning spectral and ligand field properties of monoacidopentaaminechromium (III) complexes has been accumulated.[1-7] It has been recognized that the intraconfiguration transitions can be used to determine metal-ligand bond property as well as molecular geometry. Especially the sharp-line splittings are very sensitive to the exact bond angles around the metal. Thus it is possible to extract structural information from the sharp-line electronic spectroscopy.[4,8,9]

A imidazole(imH) is biologically of especial interest because imdazole nitrogens of histidyl residues coordinate to metal ions in many metalloproteins. Thus, the identification of metal-imidazole nitrogen bond properties in biological systems provides valuable information about the structure of the active site of a metalloprotein. The method of preparation, absorption and infrared spectral data of the title compound have been reported.[10] The influence of pentaaminechromium(III) on the acidity of coordinated imidazole has also been studied.[11] However, detailed ligand field analysis of *d-d* transitions including the emission and excitation spectroscopic properties in the title complex have not been reported to date.

In this study the 77 K emission and excitation, and room temperature visible and infared spectra of $[Cr(NH_3)_5(imH)](ClO_4)_3(ClO_4)_3 \cdot H_2O$ were measured. The vibrational intervals of the electronic ground state were extracted from the far-infrared and emission spectra. The pure electronic origins were assigned by analyzing the electronic absorption and excitation spectra. Using the observed electronic transitions, a ligand field analysis has been performed to determine the metal-ligand bonding properties of the coordinated imidazole nitrogen toward chromium(III). The $[Cr(NH_3)_5(imH)]^{3+}$ complex was chosen to study the ligand field properties of imidazole nitrogen in order to keep the number of π-interacting coordinated atom to a minimum.

Experimental Section

The synthetic method of $[Cr(NH_3)_5(imH)](ClO_4)_3 \cdot H_2O$ has been reported.[11] The microcrystalline samples were generously supplied by Professor G. A. Lawrance.

The 77 K emission and excitation spectra were measured on a Spex Fluorolog-2 spectrofluorometer as describes previously.[12] The room temperature visible absorption spectrum in aqueous solution was recorded with a Hewlett-Packard 8452A diode array spectrophotometer. The mid-infrared spectrum was obtained with a Mattson Infinities series FT-IR spectrometer using a KBr pellet. The far-infrared spectrum was recorded with a Bruker 113V spectrometer. The compound was pressed into a polyethylene pellet (concentration 2 mg in 100 mg polyethylene) by using a Spex 3624B X-Press.

Results and Discussion

Far-infrared Spectrum. The vibrational intervals due to the electronic ground state can be obtained by comparing the emission spectrum with infrared spectral data. The mid-infrared absorbances of $[Cr(NH_3)_5(imH)](ClO_4)_3 \cdot H_2O$ were reported.[11] The far-infrared spectrum of this complex recorded at room temperature is presented in Figure 1.

As seen in Figure 1, the absorption band with medium intensity at 460 cm^{-1} can be assigned to Cr-N_{am} stretching mode.[13] A number of absorption bands below 350 cm^{-1} arise from lattice vibration, skeletal bending and the Cr-N_{im} stretching modes.

Emission Spectrum. The 466 nm excited 77 K emission spectrum of $[Cr(NH_3)_5(imH)](ClO_4)_3 \cdot H_2O$ is shown in Figure 2. The band positions relative to the lowest zero phonon line, R_1, with corresponding infrared frequencies, are listed in Table 1. The emission spectrum was independent of the exciting wavelength within the first spin-allowed transition region.

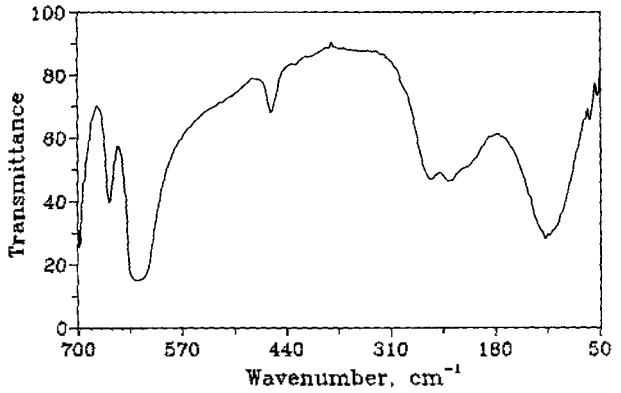

Figure 1. Far-infrared spectrum of $[Cr(NH_3)_5(imH)](ClO_4)_3 \cdot H_2O$ *in* polyethylene disk at 298 K.

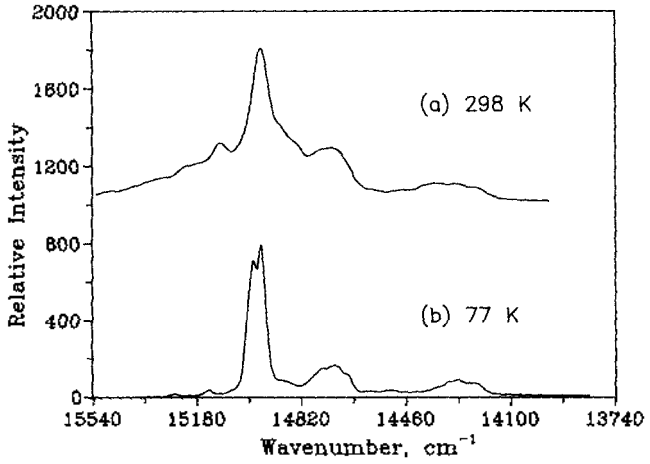

Figure 2. Emission spectrum of $[Cr(NH_3)_5(imH)](ClO_4)_3 \cdot H_2O$ from a powdered sample at 77 K (λ_{ex}=466 nm).

The strongest peak at 14950 cm^{-1} is assigned as the zero-phonon line, R_1, because a corresponding strong peak is found at 14945 cm^{-1} in the excitation spectrum. It accompanies a strong band at high-energy side. This high-energy band is referred as to R_1'. The small splitting of 25 cm^{-1} is attributed to inequivalent chromium sites. A well defined hot band at 15129 cm^{-1} may be assigned to the second component of the $^2E_g \rightarrow {}^4A_{2g}$ transition. The vibronic intervals occurring in the spectrum consist of several modes that can be presumed to involve primarily lattice vibration, angle-bending and Cr-N_{im} stretching modes with frequencies in the range 76-375 cm^{-1}. The band at 445 cm^{-1} can be assigned to a Cr-N_{am} stretching mode. It is worthing noting that emission spectrum at room temperature also shows the moderately intense and structured emission band at 14960 cm^{-1} associated with $^2E_g \rightarrow {}^4A_{2g}$ phosphorescence in the O_h approximation. It can be compared with 14970 cm^{-1} for the closely related pentaammine(pyridine)chromium(III) complex.[14]

Table 1. Vibrational frequencies from the 77 K emission and 298 K infrared spectra of $[Cr(NH_3)_5(imH)](ClO_4)_3 \cdot H_2O$[a]

Emission[b]	Infrared	Assignment
-279 w		$-\nu_4$
-179 m		R_2
-25 m		R_1'
0 vs		R_1
76 sh	53 vw, 62 vw	
	117 s	Lattice vib.,
214 w	214 sh, 238 m	skeletal bends
257 m	260 m	and
294 sh		ν(Cr-N_{im})
375 w	350 w	
445 m	460 m	ν(Cr-N_{am})
544 vw		
	625 vs	ClO_4^-
675 m	660 m	
728 w	756 s	δ(Cr-NH)

[a] Data in cm^{-1}. [b] Measured from zero-phonon line at 14950 cm^{-1}.

Excitation Spectrum. The 77 K excitation spectrum is shown in Figure 3. It was recorded by monitoring a relatively strong vibronic peak in the luminescence spectrum. The shape and peak maxima of the excitation spectrum did not vary with the vibronic peak used to monitor it. The peak positions and their assignments are tabulated in Table 2. The calculated frequencies in parentheses were obtained by using the vibrational modes ν_1-ν_6 listed in Table 2.

Two strong peaks at 14945 and 15126 cm^{-1} in the excitation spectrum are assigned to the two components (R_1 and R_2) of the $^4A_{2g} \rightarrow {}^2E_g$ transition. The lowest-energy zero-phonon line coincides with the luminescence origin within 5 cm^{-1}. The zero-phonon line in the excitation spectrum splits into two components by 181 cm^{-1}, and it can be compared with those of the chromium(III) complexes with tetragonal symmetry.[7] An experimental problem lies with the difficulty in distinguishing pure electronic components from the vibronic bands that also appear in the excitation spectrum. However, the three components of the $^4A_{2g} \rightarrow {}^2T_{1g}$ electronic origin (T_1, T_2 and T_3) are assigned to relative intense peaks at 682, 791 and 910 cm^{-1} from the lowest electronic line, R_1. Vibronic satellites based on these origins also have similar frequencies and intensity patterns to those of the ^2E_g components.

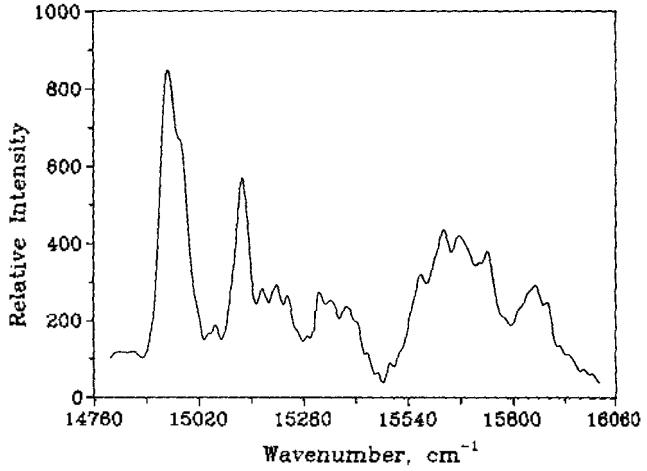

Figure 3. Excitation spectrum of $[Cr(NH_3)_5(imH)](ClO_4)_3 \cdot H_2O$ from a powdered sample at 77 K (λ_{em}=700 nm).

Table 2. Assignment of sharp-line positions in the 77 K excitation spectrum of $[Cr(NH_3)_5(imH)](ClO_4)_3 \cdot H_2O$[a]

$\bar{\nu}_0$-14945	Assignment	(Calcd)[b]		Vibronic frequencies[c]	Ground state-frequencies[d]
0 vs	R_1		ν_1	87	76
34 sh	R_1'		ν_2	115	117
97 vw	$R_1+\nu_1$	(87)	ν_3	261	260
115 w	$R_1+\nu_2$	(115)	ν_4	289	294
181 vs	R_2		ν_5	443	445
234 w	$R_1+2\nu_2$	(230)	ν_6	544	537
266 m	$R_2+\nu_1$	(268)			
294 w	$R_2+\nu_2$	(296)			
346 vw	$R_1+\nu_1+\nu_3$	(348)			
374 w	$R_1+\nu_1+\nu_4$	(376)			
402 w	$R_1+\nu_2+\nu_4$	(404)			
440 m	$R_1+\nu_5$	(443)			
466 w	$R_2+\nu_4$	(470)			
518 w	$R_1+2\nu_3$	(522)			
549 w	$R_1+\nu_6$	(544)			
576 sh	$R_1+2\nu_4$	(578)			
626 m	$R_2+\nu_5$	(624)			
682 s	T_1				
719 m	$R_2+\nu_1+\nu_5$	(711)			
771 w	$T_1+\nu_1$	(202)			
791 s	T_2				
868 vw	$T_2+\nu_1$	(878)			
910 s	T_3				
938 sh	$T_1+\nu_3$	(943)			
971 w	$T_1+\nu_4$	(971)			
999 vw	$T_3+\nu_1$	(997)			
1029 w	$T_3+\nu_2$	(1025)			
1052 vw	$T_1+\nu_1+\nu_4$	(1058)			

[a]Data in cm^{-1}. [b]Values in parentheses represent the calculated frequencies based on the vibrational modes listed. [c]From the excitation spectrum. [d]From the emission and infared spectra.

Absorption Spectrum. Figure 4 displays the visible absorption spectrum (solid line) of $[Cr(NH_3)_5(imH)]^{3+}$ in aqueous solution at room temperature.

The one ligand field maximum at 21460 cm^{-1} (ν_1) and the other at 28250 cm^{-1} (ν_2) correspond to the $^4A_{2g} \rightarrow {}^4T_{2g}$ and $^4A_{2g} \rightarrow {}^4T_{1g}$ transitions in the O_h approximation, respectively.[15] The quartet bands have nearly symmetric profiles. In order to obtain some points of reference for the splittings of the two bands, the band profiles were fitted by using four Gaussian curves, as seen in Figure 4. The contribution from outside bands was corrected for the fine deconvolution. A deconvolution procedure on the experimental band pattern yielded maxima at 20780, 21995, 27710 and 28405 cm^{-1} for the noncubic splittings of $^4T_{2g}$ and $^4T_{1g}$. These peak positions were used as the observed spin-allowed transition energies in the ligand field optimization.

AOM Calculations. The ligand field analysis was carried out through an optimized fit of experimental to calculated transition energies. The doublet and quartet energies with the appropriate degeneracies are calculated by diagonalizing the full 120×120 secular matrix which arises from the perturbed d^3 system.[16] Eigenvalues were assigned to quartet or doublet states based on a spin analysis of the corresponding eigenfunctions. The amount of quartet character in the doublet states was estimated by comparing the eigenfunctions of the excited doublet states with and without spin-orbit coupling. The ligand field potential matrix was assumed to arise only from just the six atoms in the first coordination sphere. Although the perchlorate oxygens may also perturbate metal *d* orbitals, the extent of that interaction was judged too small to warrant any additional adjustable parameters. The π-interactions of the imidazole nitrogen with the metal ion were considered to be anisotropic. Since the metal-ligand π interaction of ammonia ligands was assumed to be negligible, the seven parameters are involved in the ligand field optimizations. The AOM parameters e_σ(imH) and e_π(imH) for the imidazole nitrogen-chromium interaction, and $e_\sigma(NH_3)$ for the ammonia nitrogen-chromium interaction and interelectronic repulsion parameters are required to fit ten experimental energies: the five $^4A_{2g} \rightarrow \{^2E_g, {}^2T_{1g}\}$ components, identified in Table 3, the four $^4A_{2g} \rightarrow \{^4T_{2g}, {}^4T_{1g}\}$ components, and the splitting of the ^2E_g state. We have varied each parameter in order to find its characteristic influence on the energy level scheme. Then we used the optimization routine for the final results. As expected, the Racah parameters do actually not influence the low-symmetry level splittings consider here. In order to reduce the parameter space to a minimum, we could use therefore in first approximation parameter values which can be obtained in first good approximation from the quartet band separation ($^4T_{1g}$-$^4T_{2g} \approx 12B$) and from the energy position of lowest doublet term (^2E_g - $^4A_{2g} \approx 9B + 3C$). Since the AOM parameters have been found to be transferable between similar compounds, $e_\sigma(NH_3)$ was well established from calculations on other monoacidopenta amminechromium(III) complexes to have a value around 7200 cm^{-1}.[5-7] However, it is noteworthy that the peptide nitrogen with sp^2 hybridization has a weak π-donor character.[17] We found that the influence of increasing zeta on the doublet pattern was relatively small. Therefore, the spin-orbit coupling parameter is set at 230 cm^{-1}. Schmidtke's π-expansion parameter τ were also included in the treatment of the interelectronic repulsion term. In Schmidtke's approximation, the electrostatic terms are modified by a factor τ for each constituent metal wavefunction that overlaps with a ligand π-orbital. The value of τ was fixed at the value 0.9925. The estimated value was based on the analysis of $[Cr(NH_3)_5CN]Cl(ClO_4)$.[6] Finally, we tried to improve the calculated energy level scheme by using a fitting procedure which is based on the Powell parallel subspace algorithm.[18] The results of the optimization and the parameter set used to generate the best-fit energies are listed

Table 3. Experimental and calculated electronic transition energies for $[Cr(NH_3)_5(imH)](ClO_4)_3 \cdot H_2O$[a]

State(O_h)	Expt	Calcd[b]
^2E_g	14945	14948
	15126	15127
$^2T_{2g}$	15627	15414
	15736	15500
	15855	15589
$^4T_{2g}$	20780[c]	21011
	21995[c]	21580
$^4T_{1g}$	27710[c]	27895
	28405[c]	28590

[a]Data in cm^{-1}. [b]$e_\sigma(imH)$=6565, $e_\pi(imH)$=-532, B=637, C=3495, τ=0.9925. Fixed values: $e_\sigma(NH_3)$=7200, ζ=230. [c]Obtained from the Gaussian component deconvolution.

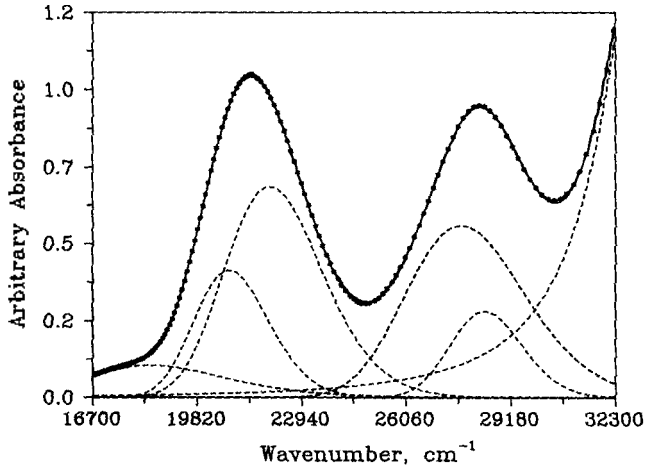

Figure 4. Electronic absorption spectrum of $[Cr(NH_3)_5(imH)]^{3+}$ in aqueous solution at 298 K.

in Table 3. The quartet terms were given a very low weight to reflect the very large uncertainty in their position.[19]

The AOM results are plausible and reproduce the spectrum pretty well. The following values were finally obtained for the ligand field parameters: $e_\sigma(imH)$=6565±23, $e_\pi(imH)$= -532±13, B=637±2, C=3495±4 cm^{-1}. The value of 6565 cm^{-1} for $e_\sigma(imH)$ is comparable to the values for other ligands such as amine nitrogens and halides.[20-26] The AOM parameters for imidazole ligand indicate that the imidazole nitrogen has medium σ-donor and net π-acceptor properties toward chromium(III) ion. The negative value of -532 cm^{-1} for $e_\pi(imH)$ can be comparable to the -890 cm^{-1} of cyanide ligand.[6] The $e_\pi(imH)$ parameter still denotes a considerable degree of π back-donation. The AOM parameters can be used for predicting the photolabilization mode and interpreting the photostereochemistry in the substitution reaction of the chromium(III) complexes.[27] An orbital population analysis yields a configuration of $(xy)^{1.009}(xz)^{0.947}(yz)^{1.027}(x^2-y^2)^{0.011}(z^2)^{0.016}$ for the lowest component of ^2E_g state. The relative d-orbital ordering from the calculation is $E(xz) \approx E(xz)$ =-533 cm^{-1} < $E(xy)$ = 0 cm^{-1} < $E(z^2)$ = 20967 cm^{-1} < $E(x^2-y^2)$ =21600 cm^{-1}. The value of Racah parameter, B is about 70 % of the value for a free chromium(III) ion in the gas phase. We also can see that the ligand field theory reproduces experimentally observed large splitting of 181 cm^{-1} of ^2E_g (O_h) state.

Acknowledgement. The author wishes to thank Professor G. A. Lawrance for a gift of the title compound. My sincere thanks are due to Professor H. U. Güdel, University of Bern, Switzerland for giving me the opportunity to visit his laboratory. Financial support of the Korea Science & Engineering Foundation and Swiss National Science Foundation is also gratefully acknowledged.

References

1. Risen, H. *Inorg. Chem.* **1988**, *27*, 4677.
2. Schmidtke, H. H.; Adamsky, H.; Schönherr, T. *Bull. Chem. Soc. Jpn.* **1988**, *61*, 59.
3. Risen, H.; Krausz, E.; Dubicki, L. *J. Lumin.* **1989**, *44*, 97.
4. Lee, K. W; Hoggard, P. E. *Inorg. Chem.* **1992**, *30*, 264.
5. Schönherr, T.; Wiskemann, R.; Mootz, D. *Inorg. Chim. Acta* **1994**, *221*, 93.
6. Schönherr, T.; Itoh, M.; Urushiyama, A. *Bull. Chem. Soc. Jpn.* **1995**, *68*, 594.
7. Schönherr, T. *Top. Curr. Chem.* **1997**, *191*, 87.
8. Hoggard, P. E. *Coord. Chem. Rev.* **1986**, *70*, 85.
9. Hoggard, P. E. *Top. Curr. Chem.* **1994**, *171*, 114.
10. Winter, J. A.; Caruso, D. : Shepherd, R. E. *Inorg. Chem.* **1966**, *5*, 1308.
11. Curtis, N. J.; Lawrance, G. A. *Inorg. Chim. Acta* **1985**, *100*, 275.
12. Choi, J. H. *Bull. Korean Chem. Soc.* **1993**, *14*, 118.
13. Choi, J. H.; Oh, I. G. *Bull. Korean Chem. Soc.* **1993**, *14*, 348.
14. Riccieri, P.; Zinato, E. *Inorg. Chem.* **1996**, *35*, 974.
15. Lever, A. B. P. *Inorganic Electronic Spectroscopy*; Elsevier: Amsterdam, **1984**.
16. Smith, B. T.; Boyle, J. M.; Dongarra, J. J.; Garbow, B. S.; Ikebe, Y.; Klema, V. C.; Moler, C. B. *Matrix Eigensystem Routines-EISPACK Guide*; Spring-Verlag: Berlin, **1976**.
17. Choi, J. H.; Hoggard, P. E. *Polyhedron* **1992**, *11*, 2399.
18. Kuester, J. L.; Mize, J. H. *Optimization Techniques with Fortran*; McGraw-Hill: New York, **1973**.
19. Clifford, A. A. *Multivariate Error Analysis*; Wiley-Hasted: New York, **1973**.
20. Choi, J. H. *Bull. Korean Chem. Soc.* **1994**, *15*, 145.
21. Choi, J. H. *J. Korean Chem. Soc.* **1995**, *39*, 501.
22. Choi, J. H. *J. Photosci.* **1996**, *3*, 43.
23. Choi, J. H. *J. Photosci.* **1997**, *4*, 121.
24. Choi, J. H.; Oh, I. G. *Bull. Korean Chem. Soc.* **1997**, *18*, 23.
25. Choi, J. H. *Bull. Korean Chem. Soc.* **1997**, *18*, 819.
26. Choi, J. H. *Bull. Korean Chem. Soc.* **1998**, *19*, 575.
27. Vanquickenborne, L. G.; Ceulemans, A. *Coord. Chem. Rev.* **1983**, *48*, 157.